Available online at www.sciencedirect.com
ScienceDirect
Tetrahedron: Asymmetry
Tetrahedron: *Asymmetry* 17 (2006) 2649–2653

Increasing the enantioselectivity of cyclopentanone monooxygenase (CPMO): profile of new CPMO mutants

Christopher M. Clouthier and Margaret M. Kayser*

Department of Physical Sciences, University of New Brunswick, Saint John, NB, Canada E2L 4L5

Received 11 August 2006; accepted 1 October 2006

Abstract—A series of cyclohexanones substituted at the 4-position with a selection of hydrophobic and hydrophilic groups were used as substrates in the evaluation of six new cyclopentanone monooxygenase (CPMO) mutants. These mutants were obtained through evolutionary modifications in two specific regions of the CPMO's putative active site. Several mutant enzymes with improved enantioselectivity were identified. Analysis of the results, in terms of a diamond model, illustrates how a family of cyclohexanone substrates may be used to explore putative active sites of Baeyer–Villiger monooxygenases (BVMOs) and to design productive mutations for specific substrates.

1. Introduction

Baeyer–Villiger oxidation is one of the key reactions in the synthetic repertoire;[1] therefore, finding safe and environmentally friendly reagents to carry it out preoccupies many 'green' chemists.[2] Apart from environmental concerns, the regio- and stereoselective carbon–carbon bond cleavage in this oxidation has been the focus of many chemical[3] and enzymatic[4] studies. Although progress has been made in 'chemical' oxidation methods, the need for selective 'green' methods has encouraged the search for biological equivalents. Numerous bacteria and fungi harbour enzymes catalyzing Baeyer–Villiger oxidations.[4] In these microorganisms, Baeyer–Villiger oxidations are part of catabolic pathways for non-carbohydrate ketones used as carbon and energy sources;[5] some of these enzymes possess remarkably flexible substrate tolerance.[4]

Cyclohexanone monooxygenase (CHMO) from *Acinetobacter* sp. NCIB 9871[6] and cyclopentanone monooxygenase (CPMO) from *Commamona* sp. NCIMB 9872[7] belong to the above category. Both enzymes transform a broad variety of the same ketones, but whereas wild-type CHMO (WT-CHMO) is often highly enantioselective[4] the wild-type CPMO rarely is.[8,9] To improve the enantioselectivity of the wild-type CPMO (WT-CPMO), we designed and carried out mutations restricted to four specific amino acid residues.[10] The selection of the mutation points was guided by the information obtained from the directed evolution of WT-CHMO.[11] Over the course of our 'mini evolution',[10] two small mutant libraries were generated using the 'casting' technique.[12] The screening of 300 mutants (150 per Library) was carried out with three probe-compounds: two substrates that can be readily oxidized by WT CPMO, but with low selectivities; a nonpolar 4-methyl-cyclohexanone **1a**, polar 4-acetoxycyclohexanone **1i**, and *t*-butyl cyclohexanone **1d** that is not accepted by the wild-type enzyme. During the initial screening we did not find mutants capable of converting *t*-butylcyclohexanone **1d**; however, mutants with improved enantioselectivities for the two remaining compounds were identified.[10] In this paper, we explore the potential of the selected six mutants as Baeyer–Villiger oxidants for a series of compounds shown in Scheme 1.

2. Results and discussion

The design and preparation of CPMO mutants used in this study were reported previously,[10] as was the synthesis of substrates and the characterization of product lactones, including their absolute configurations.[13–15] The screenings and scaled-up reactions were performed with growing cultures (log phase) in shake-flask fermentations on a 20 and

* Corresponding author. Tel.: +1 506 648 5576; fax: +1 506 648 5948; e-mail: kayser@unbsj.ca

0957-4166/$ - see front matter © 2006 Elsevier Ltd. All rights reserved.
doi:10.1016/j.tetasy.2006.10.001

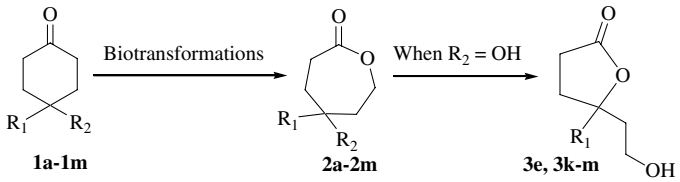

1a	R_1 = H	R_2 = Me
1b	R_1 = H	R_2 = Et
1c	R_1 = H	R_2 = Pr
1d	R_1 = H	R_2 = t-Bu
1e	R_1 = H	R_2 =OH
1f	R_1 = H	R_2 = OMe
1g	R_1 = H	R_2 = OEt
1h	R_1 = H	R_2 = OAllyl
1i	R_1 = H	R_2 = OAc
1j	R_1 = H	R_2 = COOEt
1k	R_1 = Me	R_2 = OH
1l	R_1 = Et	R_2 = OH
1m	R_1 = Allyl	R_2 = OH

Scheme 1.

100 mg scale, respectively. The conversion of substrates was monitored by GC, and the product composition was established by chiral phase GC using previously established temperature programs that allow baseline resolution for the enantiomeric lactones.[14] It should be noted that 4-OH substituted lactones **2e**, **2l**, **2k**, and **2m** rearrange spontaneously to the corresponding γ-butyro-lactones **3** as shown in Scheme 1. The extended profiling of the six mutants produced several hits, particularly in Library B created from the mutations at 156/157 positions (Table 1).

The stereoselectivity of the WT-CHMO is almost always high; this is not the case, however, for the WT-CPMO, which has an impressive substrate tolerance but usually a

Table 1. Baeyer–Villiger oxidations of 4-substituted cyclohexanones to the corresponding lactones catalyzed (growing conditions) by WT-CPMO and six mutants

Library A (449/450)	Lactonic products **2** and **3**[a]			
Substrates **1a**–**m** (R_1/R_2)	WT-CPMO Conv.% (ee%)	GlyPhe → SerTyr	GlyPhe → GlyIle	GlyPhe → GlyCys
Me/H	100 (46*R*)	27 (65*R*)	74 (92*R*)	37 (68*R*)
Et/H	100 (32*S*)	32 (35*S*)	66 (22*S*)	79 (21*S*)
Pr/H	100 (36*S*)	36 (5*S*)	81 (23*S*)	95 (24*S*)
OH/H	100 (89*S*)	NR	100 (69*S*)	NR
OMe/H	100 (28*S*)	91 (44*R*)	100 (43*S*)	96 (49*S*)
OEt/H	100 (37*R*)	92 (77*R*)	94 (27*R*)	100 (25*R*)
OAllyl/H	100 (53*S*)	8 (ND)	94 (50*S*)	20 (57*S*)
OAc/H	81 (5*S*)	20 (59*R*)	100 (8*R*)	89 (13*S*)
COOEt/H	100 (64*R*)	20 (90*R*)	76 (82*R*)	69 (78*R*)
OH/Me	81 (85*S*)	NR	NR	NR
OH/Et	92 (44*S*)[b]	NR	NR	NR
OH/Allyl	63 (52*S*)[b]	NR	NR	NR
Library B (156/157)	Lactonic products **2** and **3**[a]			
Substrates **1a**–**m** R_1/R_2	WT-CPMO Conv.% (ee%)	PheGly → LeuPhe	PheGly → AsnTyr	PheGly → HisLeu
Me/H	100 (46*R*)	89 (91*R*)	67 (88*R*)	69 (80*R*)
Et/H	100 (32*S*)	84 (90*R*)	55 (59*R*)	85 (88*R*)
Pr/H	100 (36*S*)	94 (89*R*)	44 (58*R*)	22 (59*R*)
OH/H	100 (89*S*)	23 (81*S*)	NR	NR
OMe/H	100 (28*S*)	53 (75*R*)	39 (66R)	31 (70*R*)
OEt/H	100 (37*R*)	77 (95*R*)	61 (92*R*)	56 (90*R*)
OAllyl/H	100 (53*S*)	23 (>90*R*)	22 (52*R*)	14 (ND)
OAc/H	81 (5*S*)	10 (ND[2])	19 (90*R*)	55 (74*R*)
COOEt	100 (64*R*)	56 (72*R*)	39 (78*R*)	48 (79*R*)
OH/Me	81 (85*S*)[b]	NR	NR	NR
OH/Et	92 (44*S*)[b]	NR	NR	NR

NR: no reaction; ND: not determined.

[a] The absolute configurations of all lactonic products have been previously established (see Refs. 10,13–15 and references therein).

[b] Absolute configuration was assigned by analogy to lactone **3k**.

rather lacklustre selectivity profile. We expected that a comparison of these two Baeyer–Villiger monooxygenases (BVMOs) and their mutants might lead to understanding of the differences in enantioselectivity. The strategy of introducing CPMO's mutations at positions corresponding to the 'hot spots' discovered in the evolution of CHMO[10] turned out to be profitable and led to identification of several highly selective mutants. They also provided insight into the mechanism of monooxygenase selectivity.

The X-ray analysis of PAMO, the first and only BVMO to date that produced suitable crystals, was a major development in the area of BVMOs.[16] Malito et al.[16] revealed another important fact about the monooxygenase structure; Arg-337, which occupies a position close to FAD, was shown to be essential in the substrate oxidation step. In a closely related enzyme, 4-hydroxyacetophenone monooxygenase (HAPMO), mutation of the corresponding Arg residue to Ala resulted in a complete loss of activity.[17] Arg-337's position directly in front of the flavin suggested that it may be there to stabilize the peroxide ion. In this scenario, however, when a ketone interacts with the peroxide, Arg-337's side chain must shift away to make a place for the substrate. Thus, the position of Arg-337 may be an element controlling substrate acceptance and stereoselectivity.

The crystal structure of PAMO allowed the construction of homology models for CHMO and CPMO. Sequence alignment of CHMO and CPMO with PAMO showed a very high homology (39% and 40%, respectively), suggesting that the structures of these monooxygenases should be highly conserved. Structural models constructed using CPHmodels 2.0 server[18] confirmed that the cores of the three proteins were almost identical[10] and that the Arg-337's position was highly conserved on the *re*-side of the flavin ring in CHMO and CPMO. These findings pinpointed the site of substrate binding in CPMO and CHMO. Sequencing of the eight mutants with the highest increases in enantioselectivity, obtained in the directed evolution of CHMO, identified residues 143, 432, 426, and 505 (CHMO numbering) as the 'hot spots'-positions.[11] In the 3-D homology models of several BVMOs, including CHMO and CPMO, these residues are all in proximity to the *re*-face of FAD and the catalytically essential[16,17] arginine (Arg 327 for CHMO and Arg 344 in CPMO).

Comparison of CHMO, CPMO, and their mutants indicate that the most profitable mutations are at the 432 residue for CHMO and at the 156/157 residues for CPMO. The mutations at the 432 position tend to improve the *S*-selectivity in CHMO,[14] while those at 156/157 improve the (*R*)-selectivity in CPMO (Table 1). These key residues are located on the opposite sides of the Arg 327/344 (CHMO and CPMO, respectively) with respect to the FAD molecule, as shown in Figure 1. During enzymatic Baeyer–Villiger oxidation, the substrate interacts with FAD peroxide to give the Criegee intermediate.[19] At that time, the arginine moves out of the position that stabilizes (and blocks) the peroxy group and shifts into a position that allows it to stabilize the negative charge on the O^- of the intermediate.[16,20]

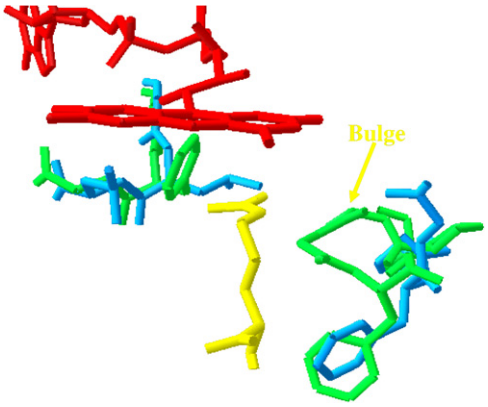

Figure 1. The positions of key residues (CHMO Phe 432 blue/CPMO Phe 450 green and CHMO Leu 143 blue/CPMO Phe 156 green) that appear to be directly involved in the stabilization of the 4-R substituent of cyclohexanone are shown in relation to FAD (red) and arginine (yellow). The homology models for CHMO and CPMO (derived from the X-ray crystal structure of PAMO[16]) show that these two pockets are antipodal with respect to the arginine.

The diamond model for stereochemical control in CHMO-catalyzed Baeyer–Villiger oxidations of cyclohexanones[15] (Fig. 2) was shown to be in agreement with the enantioselectivity changes observed in CHMO and CPMO mutants.[10,14] The application of the model (Fig. 2) suggests that suitable mutations of the 156/157 residues of CPMO may improve interactions with the 4-R substituents on cyclohexanone. Thus, configuration A is favored and the migrating bond leads to the (*R*)-lactone. The opposite is true when mutations at the residue 432 stabilize the substituent in the antipodal pocket (configuration B).

Comparison of the two regions in WT-CHMO and WT-CPMO reveals that CHMO's hydrophobic pocket with Phe432/Thr433 side chains, can accommodate/stabilize the 4-R substituent of the cyclohexanone substrate. The orientation of the 4-R group toward the Gly142/Leu143, on the other hand, is stabilized only by the interaction with the Leu143 side chain. In WT-CPMO, the two hydrophobic pockets, 156/157 and 449/450 are both Phe/Gly combinations. This means that the 4-R group of the substrate has an 'equal opportunity' to assume one or the other conformation (Fig. 1). This analysis explains why WT-CHMO is highly (*S*)-selective for cyclohexanones substituted with non-polar groups at the 4-position, and why WT-CPMO is not selective *vis-à-vis* these compounds.

A closer inspection of the homology model of CPMO (Fig. 1) shows the following sequence of amino acids: Pro447/Ala448/Gly449/Phe450. Pro447 overlaps with CHMO's Pro431 and Phe450 overlaps with CHMO's Phe432. The remaining two amino acids form a bulging loop. Excision of these two amino acids would make the CPMO hydrophobic pocket identical to that of the highly selective CHMO. Previously, Reetz et al.[20] noted an extended loop in PAMO's when this enzyme's X-ray crystal structure was compared to the homology model of CHMO. This loop, which they refer to as 'the bulge in PAMO,' was found to influence substrate acceptance and

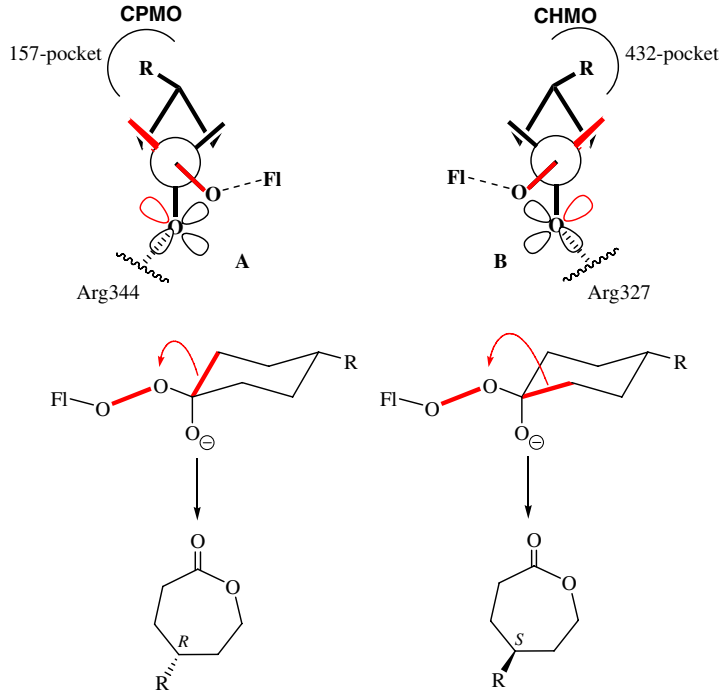

Figure 2. Mutations of residues 156/157 (CPMO) improve the interactions with the R substituents. Thus, configuration **A** is favored and the migrating bond leads to the (*R*)-lactone. The opposite is true when mutations in the 432 position (CHMO) better accommodate substituents in the antipodal pocket.

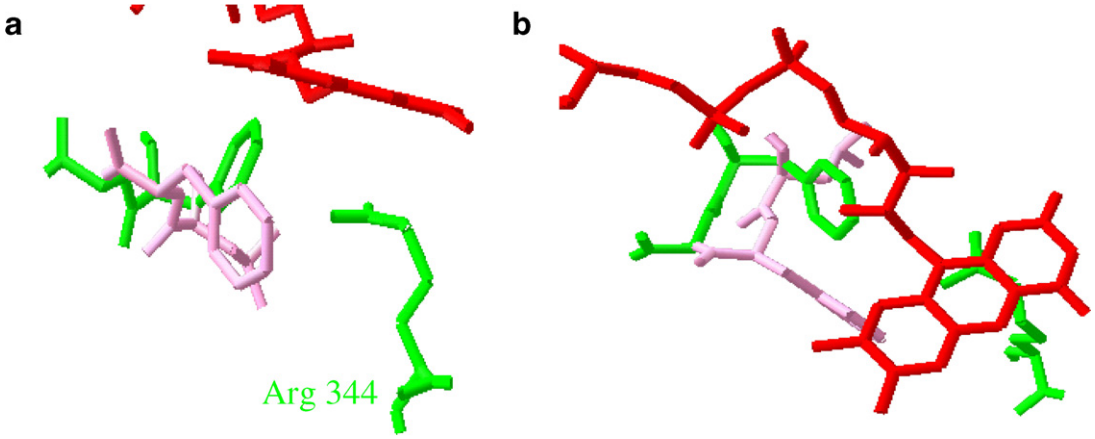

Figure 3. Improving the hydrophobic pocket of WT-CPMO by mutations at the residues 156/157 (PheGly → LeuPhe). The model shows the relative positions of FAD, Arg 344 (CPMO numbering), and 156/157 residues: WT-CPMO (Phe/Gly green) and the mutant (Leu/Phe pink), side view (a) and top view (b). The top view shows the location and character of the pocket with respect to the Arg 344 residue.

enantioselectivity. The deletion of Ser 441 and Ala 442, the two bulge residues, produced a new PAMO variant with increased substrate acceptance and enantioselectivity.[20] The existence of a similar 'bulge' in CPMO may explain why our Library A was not as successful as Library B. The effect of mutation of residues 449 and 450 may not have a full impact on the improvement of the hydrophobic pocket since the access to these amino acid residues remains blocked by the Ala 448/Gly 449 'bulge.'

The analysis of mutants from the B library indicates that the most profitable mutations produce a better hydrophobic pocket at the 156/157 location. For example, for the PheGly → LeuPhe double mutant, which gives the most dramatic enhancement of the (*R*)-selectivity for substrates **1a**–**c** (Table 1), the residue exchange appears to provide a more accommodating pocket for the 4-alkyl substituents according to the model shown in Figure 3.

3. Conclusion

In conclusion, the results listed in Table 1 show that small focused libraries of mutants, such as those generated using the casting technique can yield mutants with improved enantioselectivities. In particular, an impressive increase

in (*R*)-selectivity was observed for B-library mutants that involved mutations in the 156/157 residues. The relatively small changes in enantioselectivity observed for the A-library mutants suggest that mutations in positions 449/450 did not adequately improve the hydrophobic pocket, possibly because this location was slightly off the principal interaction(s) between the enzyme's residue(s) and the R group of the substituent. In general, the results reported here, reinforce the realization that mutations close to the active site have a higher impact on enantioselectivity, and substrate selectivity,[21] and that mutations at a residue that interacts directly with the substrate have the most profound impact. We believe that application of the diamond model in combination with modeling will provide useful blue prints for improvements in selectivity tailored for specific substrates.

4. Experimental

All chemicals were purchased from commercial suppliers and used as received. Thin-layer chromatography was performed on Sigma–Aldrich 0.2 mm aluminum-backed silica gel plates. Flash chromatography was performed on 230–400 mesh silica gel (Silicycle). Chiral-phase capillary gas chromatography was performed on either a BGB-176 (30 m × 0.25 mm × 0.10 μm) column from BGB-Analytik or a BetaDex-325 (30 m × 0.25 mm × 0.25 μm) column from Supelco. Capillary gas chromatography was performed on a DB-1301 (15 m × 0.53 mm × 1.0 μm) column from J&W Scientific.

4.1. Biotransformations with *E. coli*/CPMO, *E. coli*/CPMO mutants

The *E. coli* strains BL21(DE3)(pMM4) (or JM109(DE3)-(pET-22b)) were streaked from the frozen stock on LB-Ampicillin plates and incubated at 37 °C until the colonies were from 1 to 2 mm in size. One colony was used to inoculate 10 mL of LB-Ampicillin medium in a 50 mL Erlenmeyer flask and shaken overnight at 37 °C at 250 rpm. This culture was used at a 1:100 (v/v) ratio to inoculate an LB-Ampicillin medium supplemented with 2% glucose in a baffled Erlenmeyer flask. The culture was incubated at 37 °C, 250 rpm until OD_{600} was approximately 0.3–0.4. IPTG stock solution (200 mg/mL) was added (0.1 μL per mL of medium) and the flask was shaken for another 30 min at 24 °C. The substrate was then added; if cyclodextrin was necessary to alleviate solubility or toxicity problems, it was added at this stage. The culture was shaken at 24 °C, 250 rpm, and monitored by GC analysis until reaction was complete. The culture was then saturated with NaCl and extracted with ethyl acetate or dichloromethane. The combined extracts were washed once with brine and dried with anhydrous $MgSO_4$. The solvent was removed on a rotary evaporator and the residue was purified by flash chromatography on silica gel.

Acknowledgements

Financial support by the Natural Sciences and Engineering Research Council of Canada (M.M.K.), and the NBIF grant (M.M.K.) are gratefully acknowledged. We are grateful to Dr. C. K. Tompkins for editorial comments.

References

1. Krow, G. R. *Org. React.* **1993**, *43*, 251–296.
2. ten Brink, G.-J.; Arends, I. W. C. E.; Sheldon, R. A. *Chem. Rev.* **2004**, *104*, 4105–4123; Corma, A.; Nemeth, L. T.; Renz, M.; Valencia, S. *Nature* **2001**, *412*, 423–425.
3. Bolm, C.; Luong, T. K. K.; Schlingloff, G. *Synlett* **1997**, 1151–1152.
4. Flitsch, S.; Grogan, G. In *Enzyme Catalysis in Organic Synthesis*; Drauz, K., Waldman, H., Eds.; Wiley-VCH: Weinheim, 2002; p 1202; Stewart, J. D. *Curr. Org. Chem.* **1998**, *2*, 195–216; Iwaki, H.; Wang, S.; Grosse, S.; Bergeron, H.; Nagahashi, A.; Lertvorachon, J.; Yang, J.; Konishi, Y.; Hasegawa, Y.; Lau, P. C. K. *Appl. Environ. Microbiol.* **2006**, *72*, 2707–2720.
5. Walton, A. Z.; Stewart, J. D. *Biotechnol. Prog.* **2002**, *18*, 262–268.
6. Donoghue, N. A.; Norris, D. B.; Trudgill, P. W. *Eur. J. Biochem.* **1976**, *63*, 175–192.
7. Iwaki, H.; Hasegawa, Y.; Wang, S.; Kayser, M. M.; Lau, P. C. K. *Appl. Environ. Microbiol.* **2002**, *68*, 5671–5684.
8. Wang, S.; Kayser, M. M.; Iwaki, H.; Lau, P. C. K. *J. Mol. Catal. B: Enzym.* **2003**, *22*, 211–218.
9. Mihovilovic, M. D.; Muller, B.; Schulze, A.; Stanetty, P.; Kayser, M. M. *Eur. J. Org. Chem.* **2003**, 2243–2249.
10. Clouthier, C. M.; Kayser, M. M.; Reetz, M. T. *J. Org. Chem.* **2006**, *71*, doi:10.1021/j.0613496.
11. (a) Reetz, M. T.; Brunner, B.; Schneider, T.; Schultz, F.; Clouthier, C. M.; Kayser, M. M. *Angew. Chem., Int. Ed.* **2004**, *43*, 4075–4078; (b) Reetz, M. T.; Daligault, F.; Brunner, B.; Hinrichs, H.; Deege, A. *Angew. Chem., Int. Ed.* **2004**, *43*, 4078–4081.
12. Reetz, M. T.; Bocola, M.; Carballeira, J. D.; Zha, D.; Vogel, A. *Angew. Chem., Int. Ed.* **2005**, *44*, 4192–4196.
13. Taschner, M. J.; Black, D. J.; Chen, Q. *Tetrahedron: Asymmetry* **1993**, 1387–1390.
14. Kayser, M. M.; Clouthier, C. M. *J. Org. Chem.* **2006**, *71*, doi:10.1021/j.0613636.
15. Stewart, J. D.; Reed, K. W.; Martinez, C. A.; Zhu, J.; Chen, G.; Kayser, M. M. *J. Am. Chem. Soc.* **1998**, *120*, 3541–3548.
16. Malito, E.; Alfieri, A.; Fraaije, M. W.; Mattevi, A. *Proc. Natl. Acad. Sci. U.S.A.* **2004**, *101*, 13157–13162.
17. Kamerbeek, N. M.; Fraaije, M. W.; Janssen, D. B. *Eur. J. Biochem.* **2004**, *271*, 1–10.
18. Lund, O.; Nielsen, M.; Lundegaard, C.; Worning, P. X3M—A Computer Program to Extract 3D Models, CASP5 Conference Abstracts, 2002; p A102.
19. Sheng, D.; Ballou, D. P.; Massey, V. *Biochemistry* **2001**, *40*, 11156–11167.
20. Bocola, M.; Schultz, F.; Leca, F.; Vogel, A.; Fraaije, M. W.; Reetz, M. T. *Adv. Synth. Catal.* **2005**, *347*, 979–986.
21. Morley, K. L.; Kazlauskas, R. J. *Trends Biotechnol.* **2005**, 231–237.